Heliyon 9 (2023) e17480

Contents lists available at ScienceDirect

Heliyon

journal homepage: www.cell.com/heliyon

Analysis of NK-92 cytotoxicity in nasopharyngeal carcinoma cell lines and patient-derived xenografts using impedance-based growth method

Fatin Nur Asyiqin Abd Talib [1], Marini Marzuki [1], Susan Ling Ling Hoe [*]

Molecular Pathology Unit, Cancer Research Centre, Institute for Medical Research, National Institutes of Health, Ministry of Health Malaysia, No. 1 Jalan Setia Murni U13/15, Seksyen U13, 40170, Shah Alam, Selangor, Malaysia

ARTICLE INFO

Keywords:
Natural killer (NK) cells
Nasopharyngeal carcinoma
Co-culture
xCELLigence
Cytotoxicity

ABSTRACT

Natural killer (NK) cells are innate immune cells that can remove viral-infected tumour cells without antigen priming. This characteristic offers NK cells an edge over other immune cells as a potential therapy for nasopharyngeal carcinoma (NPC). In this study, we report how cytotoxicity was evaluated in target NPC cell lines and patient-derived xenograft (PDX) cells with effector NK-92, a commercially available NK cell line, by using xCELLigence RTCA system (a real-time, label-free impedance-based monitoring platform). Cell viability, proliferation and cytotoxicity were examined by RTCA. Cell morphology, growth and cytotoxicity were also monitored by microscopy. RTCA and microscopy showed that both target and effector cells were able to proliferate normally and to maintain original morphology in co-culture medium as they were in their own respective culture medium. As target and effector (T:E) cell ratios increased, cell viability as measured by arbitrary cell index (CI) values in RTCA decreased in all cell lines and PDX cells. NPC PDX cells were more sensitive to the cytotoxicity effect of NK-92 cells, than the NPC cell lines. These data were substantiated by GFP-based microscopy. We have shown how the RTCA system can be used for a high throughput screening of the effects of NK cells in cancer studies to obtain data such as cell viability, proliferation and cytotoxicity.

1. Introduction

Nasopharyngeal carcinoma (NPC) is a head and neck cancer that commonly afflicts the Southern Chinese and South-east Asians [1]. It has variable presence of lymphocytes and plasma cells that can reach as much as 40–50% of tumour mass [2], and is typically associated with the presence of the Epstein-Barr virus (EBV), especially in the undifferentiated carcinomas [3]. One common tumour evasion mechanism employed by EBV is to downregulate human leukocyte antigen (HLA) class I that is essential for antigen presentation-sensitization in T lymphocytes under the adaptive immune system [4].

Natural killer (NK) cells are innate tumour-infiltrating lymphocytes (TILs) capable of eradicating viral-infected tumour cells without prior recognition. This characteristic gives NK cells an edge over other immune cell types in immunosurveillance. Phenotypically, NK cells do not express CD3 (T-cell receptor); instead, CD56 is expressed with variable levels of Fc receptor, CD16. NK cells

* Corresponding author.
E-mail address: susanhoe@moh.gov.my (S.L.L. Hoe).
[1] Equal contribution.

https://doi.org/10.1016/j.heliyon.2023.e17480
Received 5 September 2022; Received in revised form 12 June 2023; Accepted 19 June 2023
Available online 25 June 2023

are activated against a broad spectrum of targets irrespective of a specific antigen expression. Activation or inhibition of NK cells depends on the fine balance of signals from activating and inhibitory receptors. Once activated, target cell death occurs via the release of lytic granules such as perforin and granzyme, induction of apoptosis by FAS ligand and TRAIL receptor, or antibody-dependent cell-mediated cytotoxicity (ADCC) [5–7].

The density of NK cells in NPC was positively correlated with better overall survival and disease progression-free survival status [2]. Interferon β-treated NK cells isolated from EBV positive NPC blood samples killed NPC cell lines and xenografts at a higher degree than untreated NK cells [8]. NK cytokilling was also reported to be sensitised by common NPC chemodrugs such as cisplatin and gemcitabine [9]. Adoptive immunotherapy using NK cells has an advantage over T-cell based therapies: faster lytic response time as activation of NK cells do not rely on prior antigen priming [10,11]. Also, as NK cells lack of surface T-cell receptors, they do not cause graft-versus-host disease in allogeneic transplants.

NK cells can be isolated from peripheral blood; however, *ex vivo* expansion is limited by poor cell quantity and purity. As such, for use in immunotherapy, NK cell-derived cytotoxic cell lines were established from patients with lymphoma. Currently, NK-92 is the only true NK cell line approved by the FDA for adoptive immunotherapy and found to possess high cytotoxicity effect on many types of tumour cells [12–14]. Other sources of NK cells include cord blood, bone marrow and induced pluripotent stem cells (iPSCs) [15]. Nonetheless, each source has its advantages and disadvantages, and possesses different phenotypic, transcriptional and functional properties.

Following the success of chimeric antigen receptor (CAR)-T cell therapies in leukaemias, NK cells are also amenable to CAR engineering, of which several clinical trials on CAR-NK from NK-92, peripheral blood, cord blood and iPSCs as the sources of NK cells, had been attempted or are on-going [16,17]. Another method to enhance NK cell cytotoxicity towards tumour cells is via natural killer cell engagers (NKCEs) [18–20]. These multifunctional antibodies target both the antigens on tumour cells as well as activating receptors on NK cells. For example, bispecific killer cell engagers (BiKEs) targeting CD16 on NK cells and tumour antigens such as EpCAM, CD133 and CD19 had been developed for use in solid tumours and non-Hodgkin's lymphomas. To improve BiKEs, trispecific killer engagers (TriKEs) targeting CD16 and a tumour antigen, crosslinked with human IL-15 to stimulate NK cell proliferation and its activation/survival, have also been reported. For a more comprehensive reading on CAR-NK, BiKEs and TriKEs, readers are encouraged to read the cited articles.

A real-time, label-free impedance-based monitoring combined with microfluidic cell culture platform allows high throughput measurements of cell viability, cytotoxicity and cellular processes such as cell proliferation and invasion-migration. Electrical impedance signals from cell adhesion are converted into arbitrary cell index (CI) values as a direct measurement of aforementioned cellular functions. The technology had been used to compare the efficacy of unmodified versus chimeric antigen receptor (CAR)-modified NK-92 cells in the treatment of neuroblastoma cells [21], to evaluate cytolytic activity of activated/unactivated NK cells with placental mesenchymal stem cells [22], and to study stimulating and inhibiting factors of NK cells isolated from peripheral blood mononuclear cells (PBMCs) [23]. Here, we explore its use to determine the dynamics of cytokilling of NPC cell lines and NPC PDX cells by NK-92 cell line.

2. Materials and methods

2.1. Cell lines and culture

HK1 was cultured in RPMI-1640 (#31800-022) supplemented with 10% fetal bovine serum (FBS) (#10082-139) and 1% penicillin/streptomycin (#15140-122) which were obtained from Gibco, USA. NPC43 and C17 were maintained in RPMI-1640 supplemented with 10% FBS, 1% penicillin/streptomycin and 4 μM Rho Kinase (ROCK) inhibitor (#SCM075) from Merck, Millipore, USA, while C666-1 was cultured in RPMI-1640 supplemented with 10% FBS, 1X GlutaMAX supplement (#35050-061) and 1% penicillin/streptomycin from Gibco, USA. Descriptions of HK1, NPC43, C17 and C666-1 cell lines can be referred in Refs. [24–27]. For co-culture image acquisition, NPC cells lines were transduced with GFP-Luc2 lentivirus vector [28] and the positive GFP-cells were sorted using a FACSAria SORP (BD Biosciences).

Human NK-92 cell line (#CRL-2407™), an interleukin-2 (IL-2)-dependent natural killer cell line derived from a patient with malignant non-Hodgkin's lymphoma, was obtained from ATCC, USA. It was cultured in Alpha Minimum Essential medium (#31800-022), supplemented with 12.5% horse serum (#16050-130), 12.5% FBS and 0.1 mM 2-mercaptoethanol (#21985-023) from Gibco, USA, 0.2 mM myo-inositol (#I7508-50G) and 0.02 mM folic acid (#F8758-25G) from Sigma Aldrich, USA and 100 U/ml Recombinant Human IL-2 (#200-02) from PeproTech.

All cells were incubated at 37 °C in a humidified atmosphere of 5% CO_2 environment.

The cell lines were periodically checked for mycoplasma contamination with e-Myco™ Mycoplasma PCR Detection Kit (#25235 from iNtRON Biotechnology Inc., Korea). To authenticate the cells, standard short tandem repeat (STR) genotyping was performed in both NPC cell lines and PDX lines for 15 STR loci plus amelogenin (gender identification).

2.2. Tissue dissociation and xenograft cell culture

Experiments with human NPC patient-derived xenograft (NPC PDX: B110 and G517) from NSG mice were performed in accordance with the protocols approved by Animal Care and Use Committee (ACUC), Ministry of Health, Malaysia (ACUC/KKM/02 (03/2017) (manuscript in preparation). Harvested NPC PDX tumours were transferred to cold PBS supplemented with 1X Pen-Strep-Fungizone (#15240-122) and processed immediately. Surrounding blood capillaries, fat, and/or necrotic tissue were removed and washed

twice with PBS with 1X Pen-Strep-Fungizone. The tumours were minced into 2 to 4-mm fragments and incubated with the appropriate dissociation solution (2 mg/mL Collagenase Type II (#C688) from Sigma-Aldrich, USA and 200 U/mL DNase I (#90083) from Thermo Fisher Scientific, USA) on a belly dancer shaker with a constant agitation for 1–2 h at 37 °C, 5% CO_2. This was followed with an addition of complete RPMI-1640 growth media supplemented with 10% FBS, 1% GlutaMAX supplement, 1X Pen-Strep-Fungizone, 1X B-27 Supplement (#17504–001), 1X Insulin-Transferrin-Selenium (ITS) (#41400–045), Fibroblast growth factor (FGF)-Basic (bFGF) (#PHG0261), Epidermal growth factor (EGF) (#PHG0311) (all were obtained from Gibco) and 10 μM ROCK Inhibitor. The entire suspension was then filtered through 40-μm nylon mesh cell strainer (BD Falcon, USA). The released cells were centrifuged at 800 rpm for 5 min. RBC lysis solution was added onto the cells prior to centrifugation. The cells were then processed with the mouse cell depletion kit (Miltenyi Biotec, Germany, #130–104-694) following the manufacturer's instruction to enrich for human NPC PDX cells by removing contaminating mouse cells. Only cells with more than 75% viability were used in the following experiments. Mycoplasma detection was similarly performed periodically as for NPC cell lines. STR profiling was also carried out on the PDX lines.

2.3. Monitoring real-time proliferation measurement and optimal seeding density

NPC cell growth and proliferation experiments were performed and monitored in real-time using the xCELLigence RTCA DP and SP system (Agilent Technologies, USA). First, 50 μl of respective cell culture medium was added to each well of E-plate and the plate was transferred to the station of RTCA system to measure background impedance. RTCA system was placed in a humidified incubator at 37 °C and 5% CO_2. In order to monitor cell growth at logarithmic phase and to determine optimal seeding density as well as time for addition of NK-92 cell for co-culture assay, three different densities (2.5×10^4, 3.0×10^4, 3.5×10^4 cells/well) of NPC cells (quadruplicate wells per cell line) were seeded into the well in a volume of 200 μl. After the cells were seeded, the E-plate was kept in biological safety cabinet for 30 min for the cells to gravitate down to the bottom of plate before being transferred back to the RTCA system. Cell impedance was monitored at 1-h time interval for 7 days and the impedance was converted to cell index (CI) value by the RTCA system. The CI value represents a quantitative measure of the growth and proliferation of the cells. The experiments were performed at least three times as recommended by xCELLigence system.

2.4. Co-culture media optimization

The co-culture media at 1:1 ratio of target cell (NPC43, HK1, C666–1, C17, B110, and G517) media and effector cell (NK-92) media was evaluated for any deleterious effect on the growth of target cells during co-culture. The target cells were first seeded into a 24- or 96-well plate in their own respective culture medium until cell attachment. Cell viability of the target cells in individual culture medium and in co-culture medium at 0 and 72 h was validated by using CellTiter-Glo (CTG; Promega, USA, #G7571), an established cell viability assay. Cell morphology was also observed by using Olympus CKX41 fluorescence microscope and bright field images were acquired at 24, 48 and 72 h.

2.5. Real-time cytotoxicity measurement of target NPC cells co-cultured with NK-92 cells (xCELLigence system)

After the optimal seeding density was determined, the dissociated target NPC cells were seeded into the E-plate in a volume of 100 μl/well and the target cells were allowed to adhere and to proliferate up to the determined time for treatment with effector NK-92 cells. When NK-92 cells were added, the impedance data acquisition was paused. One hundred microlitres of target and effector cell culture media (1:1 vol ratio) containing the effector (NK-92) were added to the target cells at a range of target:effector (T:E) ratios (1:0.25, 1:0.5, 1:1, 1:2, 1:4, 1:6, 1:8 and 1:10). The E-plate was immediately transferred back to the RTCA system. Data acquisition was monitored at 15-min time intervals for up to 72 h. Data were expressed as CI, and normalized CI values (i.e. individual CI values normalized to the CI value of T:E 1:0 at the time point of NK-92 addition). This, in turn, was converted to percentage of cytolysis and KT50 value with the RTCA Pro software. Percentage of cytolysis is calculated as: $[1 - (NCI_s)/(\text{Avg } NCI_r)] \text{ X } 100$ whereby, NCI_s is the normalized CI for the sample and NCI_r is the average of normalized CI for the matching reference wells [29]. KT50 is the amount of time it takes to kill 50% of the target cells.

2.6. Co-culture image acquisition of GFP-stained cells

The effect of NK-92 cell-mediated cytotoxicity on NPC cells was examined using an IN Cell Analyzer 2000 (GE Healthcare, USA). For co-culture image acquisition, the target NPC cells transduced with *gfp-luc2* reporter genes were seeded into a black-walled 96-well plate and treated with effector cells using the previously described experimental design. Brightfield and fluorescence images were acquired at 24 and 72 h.

2.7. Statistical analysis

Data generated from the xCELLigence system were expressed as mean ± standard deviation (SD) or standard error of mean (SEM), with at least two or three independent experiment repeats. Statistical significance was determined with One-Way ANOVA analysis using GraphPad Prism 6 (USA). Differences were considered significant when $p < 0.05$.

Fig. 1 shows the overall experimental design for this study.

3. Results

3.1. Cell proliferation and optimization of seeding density

Prior to running NK-92 cytotoxicity assay with NPC cells in the xCELLigence system, all cells were confirmed to be mycoplasma-free. The cells were also authenticated by STR profiling and found to be identical and closely related to the ones used by NPC researchers [30] (Supplementary Table 1). A cell seeding density optimization was required to establish the proliferation rate of individual target NPC cells in their respective culture medium. This step also helped to determine the optimal seeding density of target NPC cells and the time point during the logarithmic growth phase of target NPC cells for NK-92 addition in the co-culture assay.

To determine an optimal seeding density of target NPC cells to be used for the RTCA system, HK1, NPC43, C666–1 and C17 were seeded in to the E-plate in three different densities from 2.5×10^4, 3.0×10^4, 3.5×10^4 cells/well and respective impedance was determined (Fig. 2). The CI values of HK1 cells (Fig. 2A) showed a steep increase upon cell attachment and reached its highest point at 40 h post growth, while CI of NPC43 cells (Fig. 2B) continued to increase to 120 h. In contrast, both C666-1 (Fig. 2C) and C17 cells (Fig. 2D) showed an increase in growth rate up to 120 h and 168 h, respectively, albeit in a relatively slow growth proliferation rate. The growth rate of B110 (Fig. 2E) was faster than its counterpart NPC PDX, G517, although both NPC PDX cells recorded similar maximum growth at 120 h at different CI values (Fig. 2E and F). At its peak growth, the CI of B110 was two times higher than G517. Interestingly, G517 cells had rapidly attached to the E-plate and reached a maximum CI of 2 by 12 h post-seeding (Fig. 2F). This was

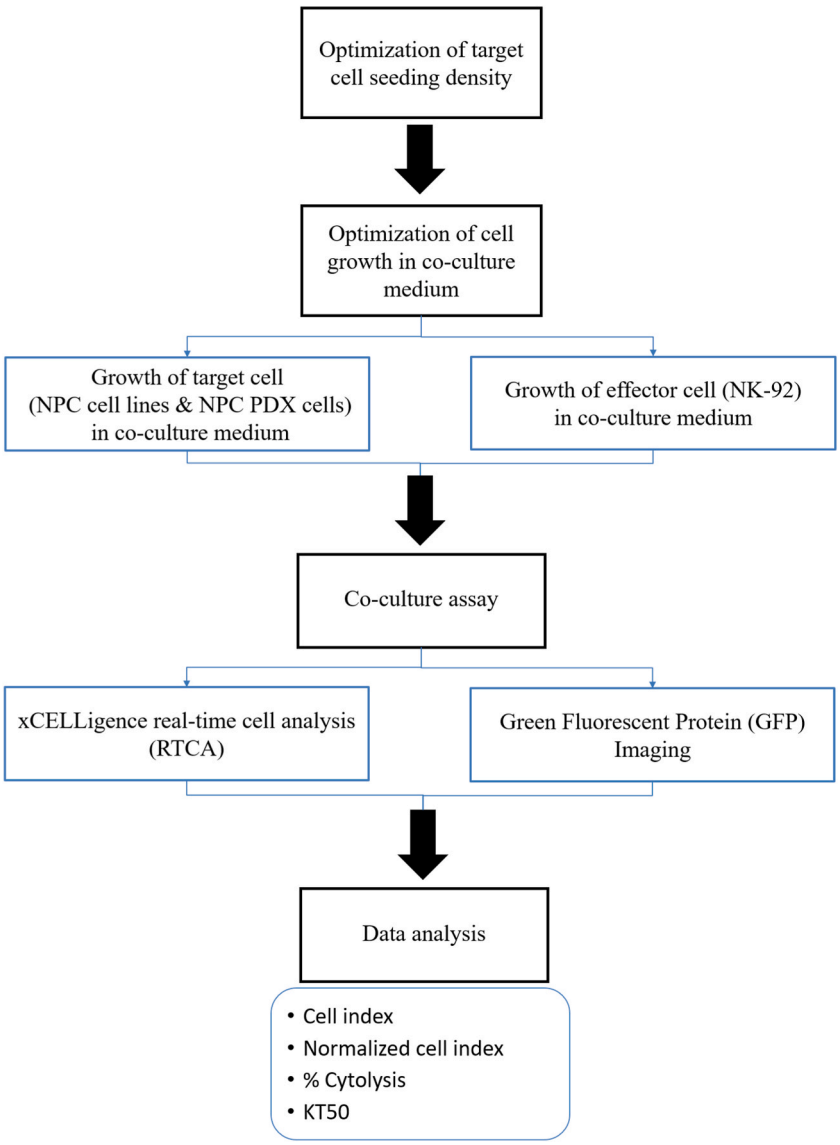

Fig. 1. Flowchart of the study.

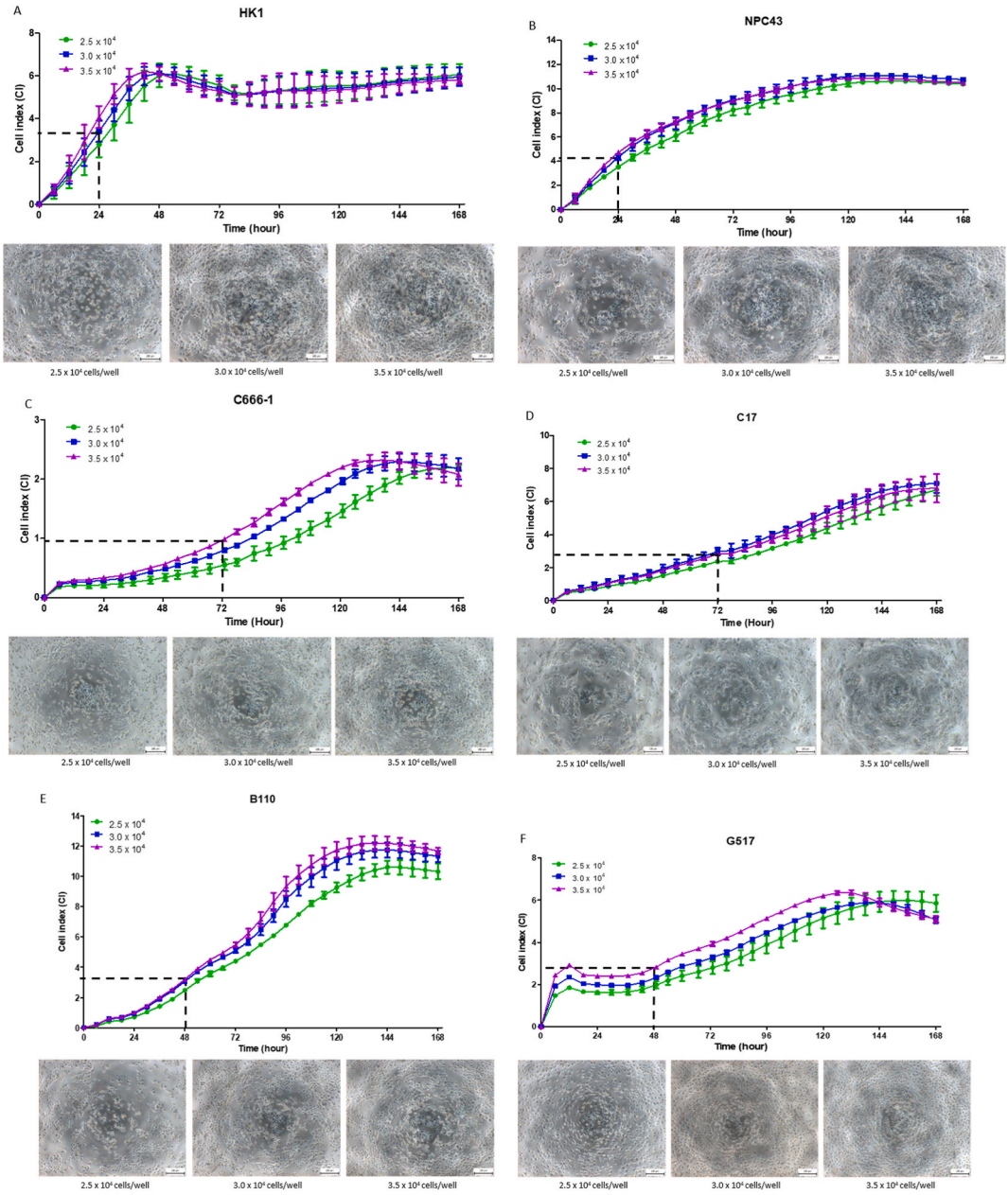

Fig. 2. Cell proliferation curve and density optimization. Three densities of NPC and NPC PDX target cells were automatically monitored every 1-h time interval over 7 days to identify a suitable seeding number and time point for addition of NK-92 cells. Results were expressed as CI values. Microscopic images of the cells after 24 h post seeding for (A) HK1, (B) NPC43; after 72 h post seeding for (C) C666-1, (D) C17; 48 h post seeding for (E) B110 and (F) G517. Results were expressed as CI ± SEM values with experimental replicates n = 2 for NPC cell line and n = 3 for NPC PDX cells. 4× objective; scale bar 200 μm.

followed by a gradual growth rate till its peak at 120 h post-seeding. The optimal seeding density for HK1 and NPC43 was determined to be 3.0×10^4 cells/well and the time point for NK-92 addition was at after 24 h seeding. Meanwhile, the appropriate time point for addition of NK-92 on C666–1 and C17 cells was at 72 h post seeding at 3.5×10^4 cells/well seeding density for the target cells. B110 and G517 were ideally seeded at 3.5×10^4 cells/well and the time point for NK-92 was at 48 h after seeding (Supplementary Table 2).

In parallel, cell morphology and attachment were observed daily using inverted microscopy with the same seeding density of target NPC cells in normal 96-well plate (Fig. 2 bottom panel of each growth curve).

3.2. Optimization of co-culture media

To investigate whether the co-culture media would give any change on cell viability, growth, proliferation and morphology of target NPC cells, CTG assay (Fig. 3A) was performed in respective individual medium and in co-culture medium. The NPC and NPC PDX cells were seeded in 24-well plate at density of 1.0×10^5 cells/well in 1 ml of individual culture medium and in co-culture medium for 72 h, similar to length of co-culture treatment in actual experiments. The effect of co-culture medium on NPC cells was observed every 24, 48 and 72 h (Fig. 3B–D). At the end of 72 h, both sets of media recorded similar increase of luminescence from cell

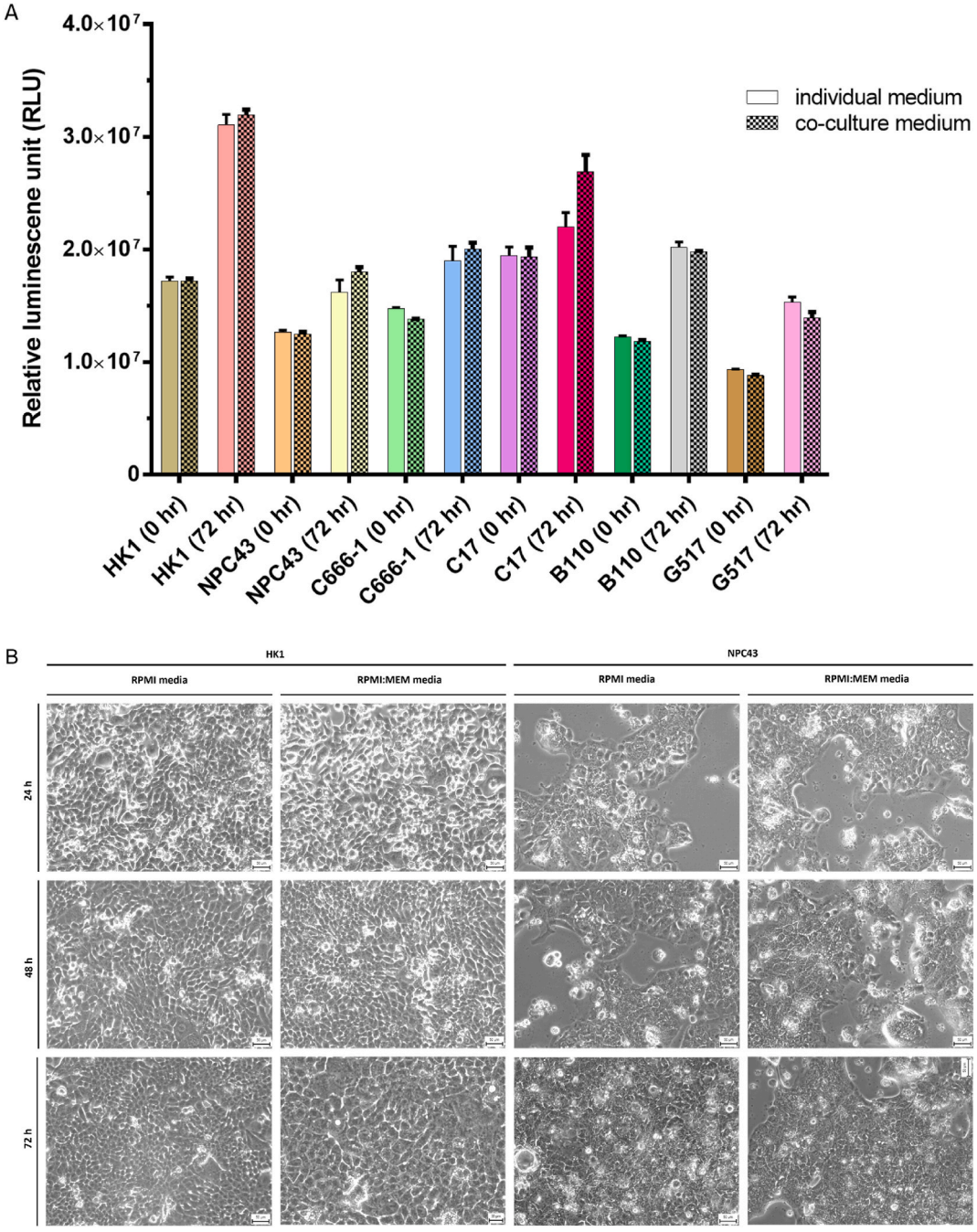

Fig. 3. Optimization of NPC and NPC PDX cells in co-culture medium. The viability of all target cells (A) in individual culture medium and in co-culture medium was measured by CTG assay, and individual HK1, NPC43 (B), C666–1, C17 (C), and B110, G517 (D) cells were morphologically observed for 72 h after the cell culture media were changed into the co-culture medium (1:1 ratio of target cell medium and effector cell medium). 10× objective; scale bar 50 μm.

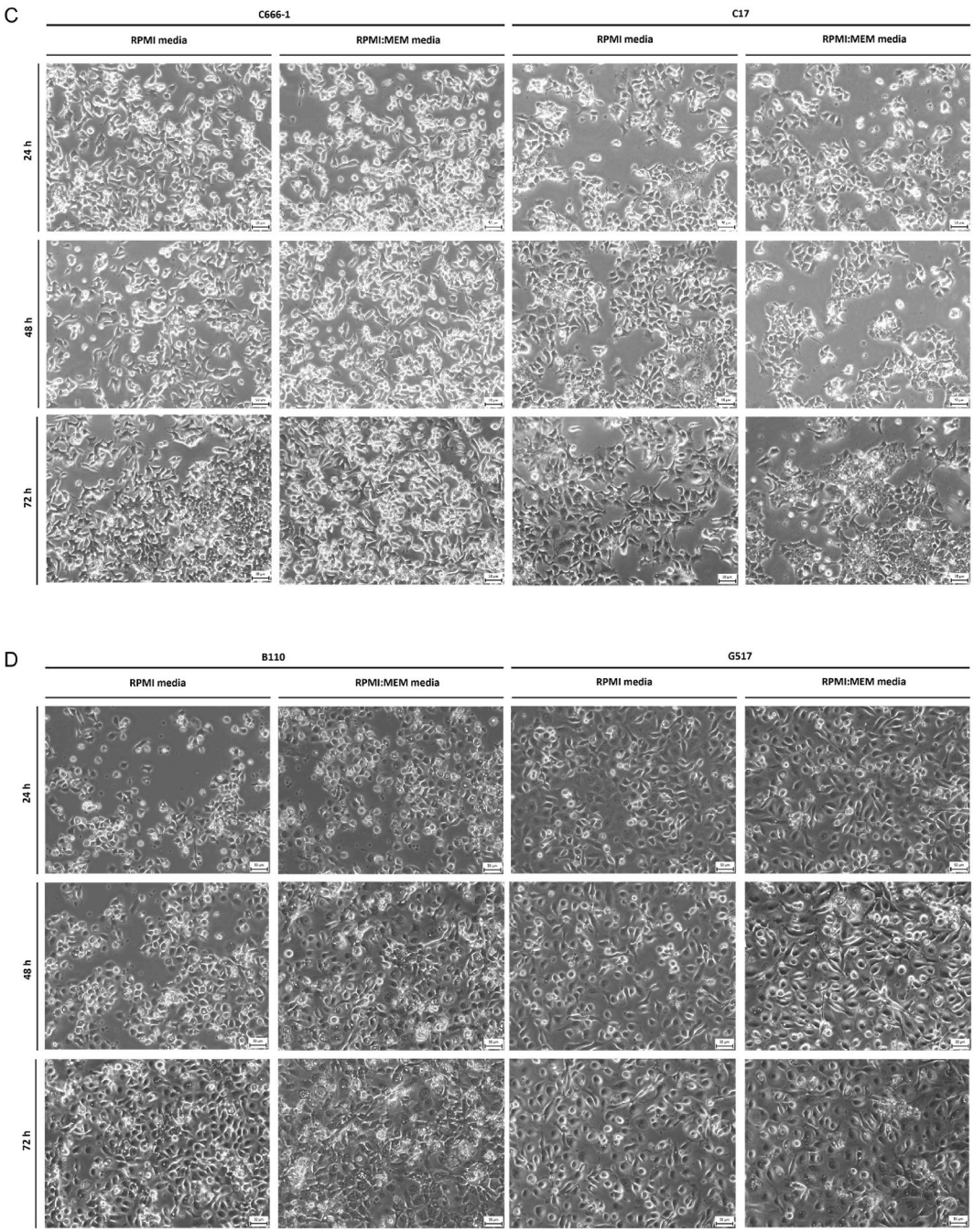

Fig. 3. (*continued*).

proliferation. Moreover, the co-culture medium did not induce any noticeable changes in the morphology of NPC nor NPC PDX cells.

Concurrently, this study also investigated whether the co-culture media would induce any change on effector NK-92 cell viability, growth and proliferation, by using CTG assay (Fig. 4A). NK-92 cells were seeded in 96-well plate at 3.0×10^4 cells/well in co-culture media for 96 h, followed by measurement of cell viability. The CTG results show that the growth and proliferation of NK-92 cells in RPMI (NPC PDX):MEM and RPMI (NPC):MEM co-culture media were comparable to its own medium (MEM) for up to 72 h, prior to a slowing growth in all three media at 96 h. Therefore, the co-culture assay was only investigated up to 72 h post-addition of NK-92. The effect of co-culture media on the morphology and proliferation rate of NK-92 cells was also observed microscopically every 24, 48 and 72 h (Fig. 4B). Here, the co-culture media did not give any apparent change in cell growth, proliferation and morphology of NK-92, as they continued to grow in their usual aggregate form as seen in MEM medium.

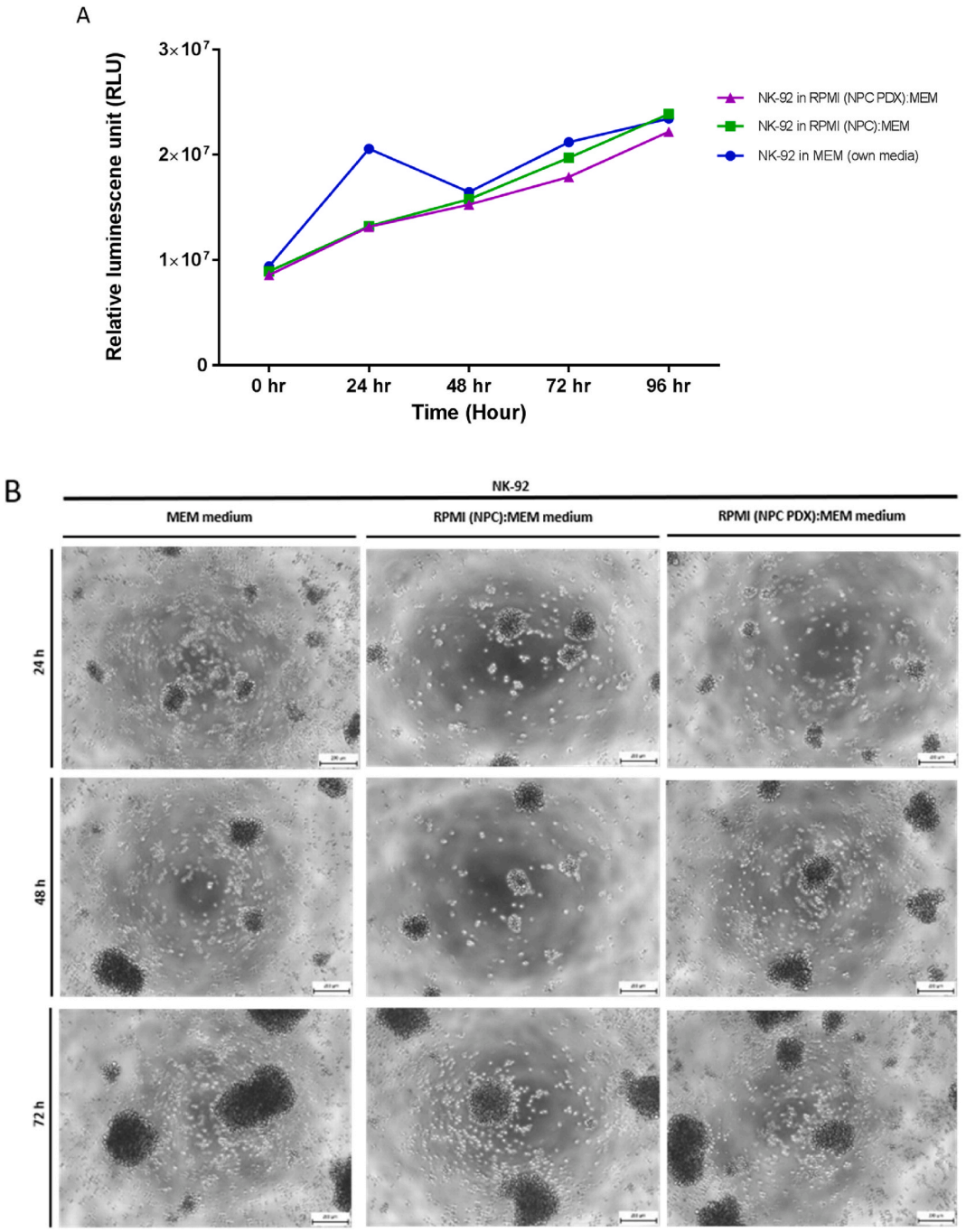

Fig. 4. Optimization of NK-92 cells in co-culture medium. (A) The viability of effector NK-92 cells was measured by CTG assay and (B) the cells were observed for 72 h once the cell culture medium was changed into the co-culture medium (1:1 vol ratio of target cell medium and effector cell medium). 4× objective; scale bar 200 μm.

3.2.1. NK-92 cytotoxicity and 50% killing target time

After determining the respective seeding density and time point of NK-92 addition for each target NPC and NPC PDX cell, different target NPC:effector NK-92 (T:E) cell ratios were co-cultured. In order to determine the real-time viability of the target NPC cells as well as the NK-92 cytotoxicity on NPC cells, target NPC cells were treated with NK-92 at T:E ratios ranging from 1:0.25 to 1:10 and were monitored using RTCA system over a period of 72 h after addition of effector cells.

Target NPC cells treated with co-culture growth media alone (T:E; 1:0) was set up as a negative control, while NK-92 cells in co-culture media alone (0:1) served to determine whether NK-92 cells were able to generate an impedance signal to the RTCA system.

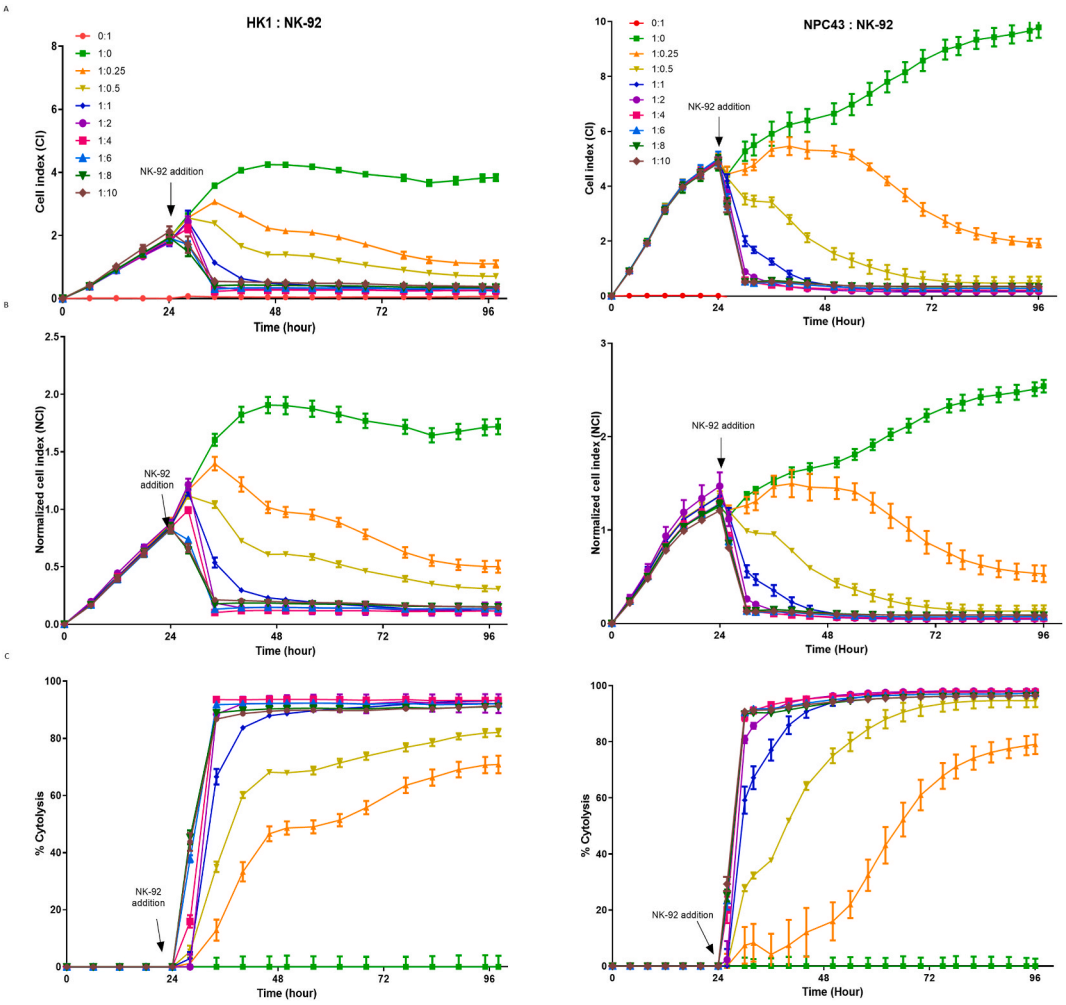

Fig. 5. Effect of co-culture of HK1 and NPC43 cells, respectively with NK-92 cells. Both HK1 and NPC43 cells were seeded in E-plate 96. NK-92 cells were added to the wells 24 h later. The rate of proliferation was monitored in real-time using xCELLigence system. (A) Cell index plot of HK1 and NPC43 target cells treated with NK-92 cell with different T:E ratios. (B) Individual CI value was normalized to the CI value of T:E 1:0 at the time point of NK-92 addition and (C) normalized CI plot converted to % cytolysis plot. Results were expressed as y ± SEM values with experimental replicates n = 2.

Figs. 5–7 show that NK-92 cells did not produce an impedance (CI ≈ 0) as NK-92 cells are non-adherent and thus, did not adhere to the gold microelectrodes of the E-plate. A clear correlation was shown between the different ratios of NK-92 cells added and resulting detectable changes of CI values. Whilst the CI value from the target NPC cells only (1:0) kept increasing up to 96 h, wells with increased target cell:NK-92 cell ratios showed an immediate and time-dependent decrease in CI values (Figs. 5–7). Supplementary Fig. 1 showed the histograms of CI values measured at 4, 24 and 72 h after NK-92 addition for the different T:E ratios. Although cytokilling in target NPC cells had occurred fast by 24 h after NK-92 addition, CI values had continued to decrease significantly at 72 h for NPC43, C666–1 and C17 at certain T:E ratios.

NK-92 cells mediated the killing of 50% of target HK1 cells in less than 50 h, and as the T:E ratio increased, its KT50 value decreased (Fig. 8). On the other hand, the KT50 of NPC43 was less than 10 h post addition of NK-92 cells at high ratios (1:1 to 1:10). Half of target C666-1 cells were killed at less than 20 h at low T:E ratios (1:0.25 and 1:0.5), and within 4 h at high T:E ratios (1:1 to 1:10). Meanwhile, lower ratios of NK-92 (1:0.25 to 1:2) needed approximately 5–30 h to eradicate 50% of target C17 cells, before an accelerated KT50 was reached at higher C17:NK-92 ratios of 1:4 to 1:10. Half of both target B110 and G517 cells were killed within 4 h of NK-92 addition. Generally, as the T:E ratios increased, a shorter KT50 was needed to eradicate the target NPC cells. Also, amongst the NPC cell lines, HK1 was the most resistant to NK-92 killing.

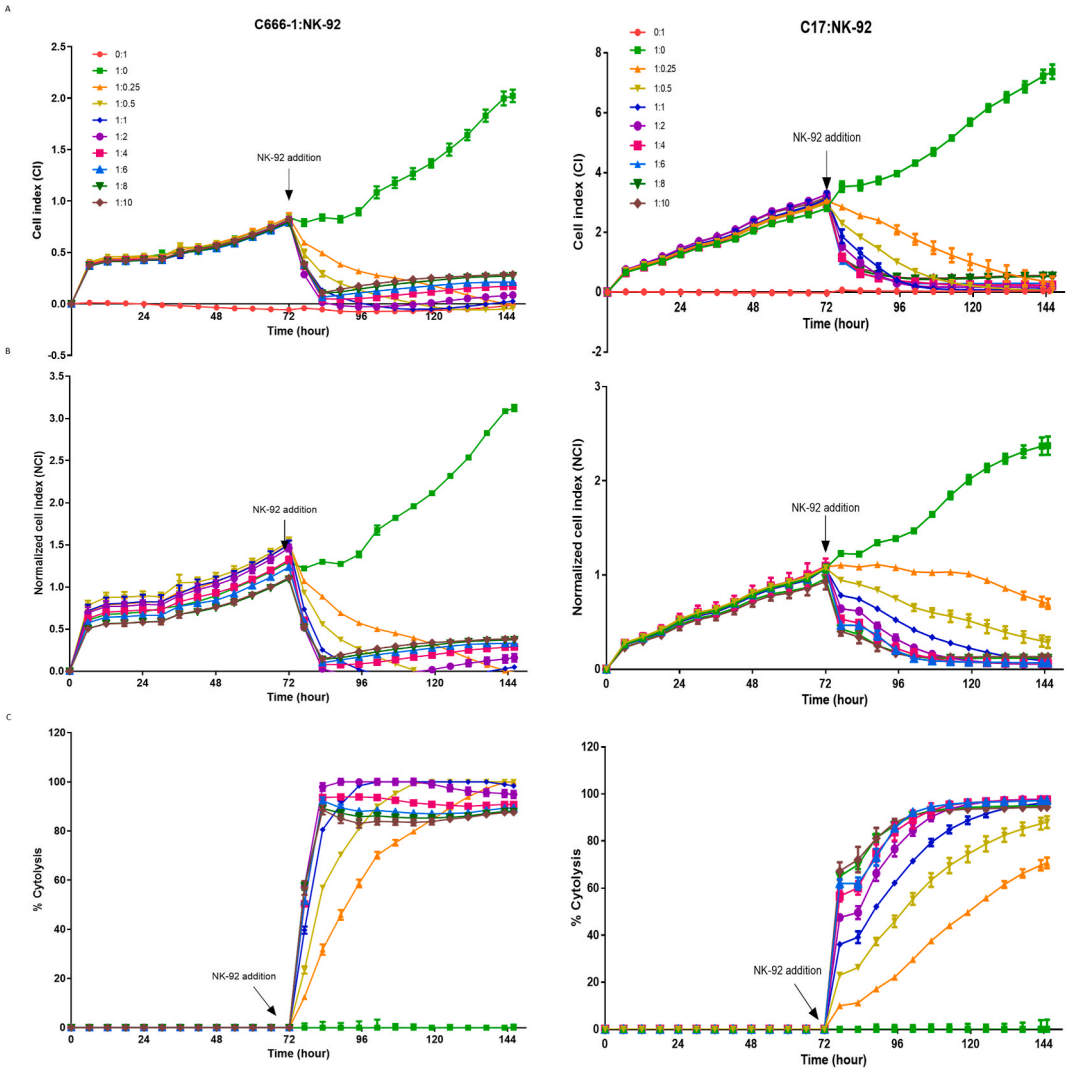

Fig. 6. Effect of co-culture of C666–1 and C17 cells, respectively with NK-92 cells. Both C666–1 and C17 cells were seeded in E-plate 96. NK-92 cells were added to the wells 72 h later. The rate of proliferation was monitored in real-time using xCELLigence system. (A) Cell index plot of C666–1 and C17 target cells treated with NK-92 cell with different T:E ratios. (B) Individual CI value was normalized to the CI value of T:E 1:0 at the time point of NK-92 addition and (C) normalized CI plot converted to % cytolysis plot. Results were expressed as y ± SEM values with experimental replicates n = 2.

3.3. Co-culture image acquisition

In order to visualize NK-92 killing the target NPC cells and the effect of this killing in the NPC cells at various T:E ratios, a parallel experiment of NPC cells transduced with *gfp-luc2* reporter genes (NPC GFP-Luc 2 cells) were co-cultured with NK-92 cells. By using IN Cell Analyzer 2000, cell morphology changes were monitored by acquisition of fluorescence images of GFP at 24 and 72 h (Fig. 9; Supplementary Fig. 2). As GFP positive images denote viable NPC cells, acquired images demonstrated that majority of target NPC cells were still viable at lower T:E ratios. Overall, the images corroborated with above data acquired by xCELLigence system that showed NPC cells were killed at a T:E ratio-dependent manner, which were evidently seen in HK1 and NPC43.

4. Discussion

In this study, we have presented a detailed methodology of using xCELLigence, a real-time cell analysis (RTCA) technology, to ascertain cell-mediated cytotoxicity in co-culture experiments of a well-known effector natural killer cell line (NK-92), and target NPC cells (cell lines as well as PDX cells). We show that the overall individual growth and morphology of these different cell types was unaffected by the co-culture media per se. NPC PDX cells (B110 and G517) were more sensitive to NK-92 cytotoxicity, even at the lowest T:E ratio of 1:0.25, compared to NPC cell lines (HK1, NPC43, C666–1 and C17). Data captured by xCELLigence were

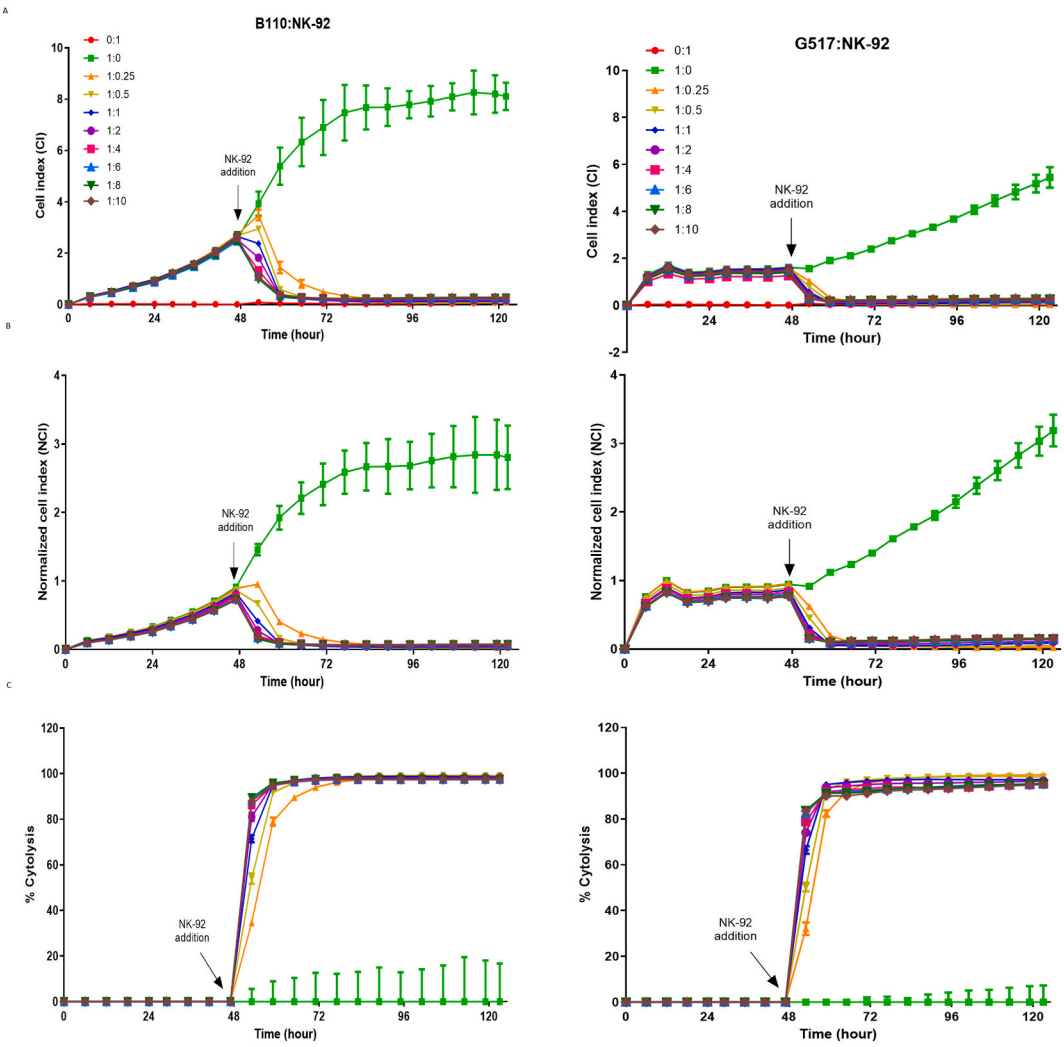

Fig. 7. Effect of co-culture of B110 and G517 cells, respectively with NK-92 cells. Both B110 and G517 cells were seeded in E-plate 96. NK-92 cells were added to the wells 48 h later. The rate of proliferation was monitored in real-time using xCELLigence system. (A) Cell index plot of B110 and G517 target cells treated with NK-92 cell with different T:E ratios. (B) Individual CI value was normalized to the CI value of T:E 1:0 at the time point of NK-92 addition and (C) normalized CI plot converted to % cytolysis plot. Results were expressed as y ± SEM values with experimental replicates n = 2.

recapitulated by microscopic images of viable GFP-transduced NPC cells.

xCELLigence platform provides real-time quantitative data of cell numbers, cell adhesion and/or morphology in the form of an arbitrary measurement of cell index (CI). When CI values are plotted against time intervals of observation, a cell proliferation profile can be obtained to identify logarithmic growth phase of target cells for cytotoxicity experiments, as shown in Results. Although it is a newer technology using arbitrary numbers to represent cell proliferation/viability values, its data had been shown to be strongly correlated with those acquired by conventional cell proliferation/viability assays such as WST-1 and CSFE [31,32]. Likewise, NPC cells (without NK-92) showed positive proliferation trends in co-culture media throughout 72 h as measured by CTG assay (Fig. 3A) and xCELLigence platform (Figs. 5A–7A) in this report. The key advantages of this technology are it is label-free which allows for more physiological-like experiment conditions, there is real-time acquisition of data collection, in addition to no/minimal user interaction which reduces technical variations in between experiments. Its main disadvantage is the equipment can only be fitted with its own brand of E-plates for experiments due to the proprietary nature of its technology. Although a basic xCELLigence equipment can be used for performing co-culture experiments, it requires a different analytical software for measurements of various calculations of cytolysis and displays of T:E ratios (RTCA Software Pro; to be purchased, or downloaded free for a trial period). For a more comprehensive review of RTCA technology, readers are advised to refer to Stefanowicz-Hajduk and Ochocka [33].

Whilst xCELLigence was primarily developed for adherent cells, one group had successfully treated the plate surface with extracellular matrix such as fibronectin and laminin to attract the adhesion of suspending leukaemia/lymphoma cells onto the plate [34]. Following this, cytotoxicity results obtained by xCELLigence were similar to conventional MTT assay. In NPC studies, xCELLigence was

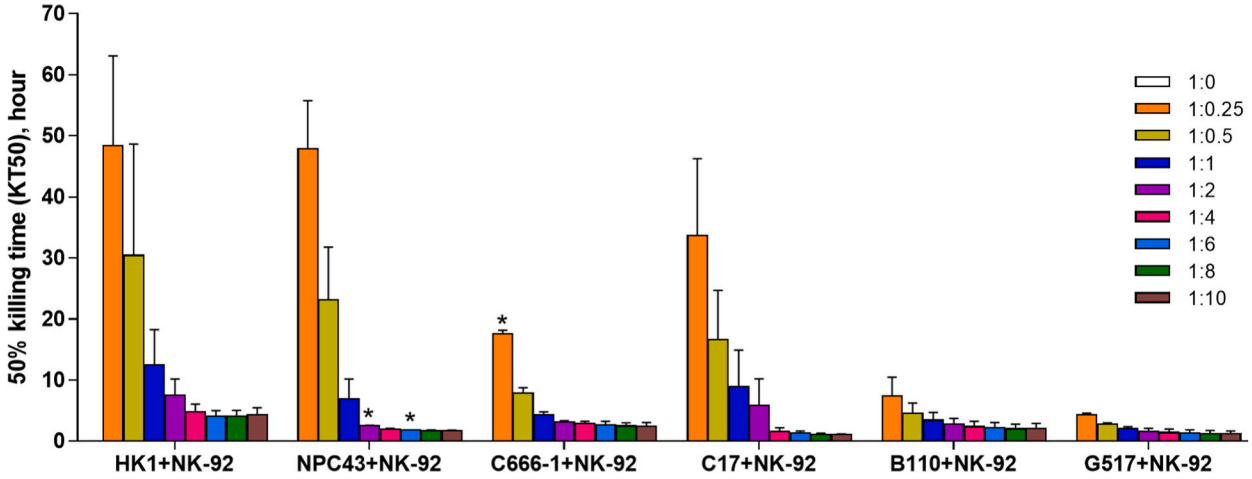

Fig. 8. Overall NK-92 cytotoxicity effect in NPC cell lines and PDXs. 50% killing time (KT50) of target cells was measured by the RTCA Pro software. Results were expressed as KT50 ± SEM values with experimental replicates n = 2 or 3. T:E ratio of 1:0 is unattainable. One-Way ANOVA result indicates significant difference between individual T:E ratio with control group (T:E 1:0) (*$p < 0.05$).

commonly used to monitor cellular processes such as proliferation, migration and invasion [35–37]. A recent immunotherapy publication used xCELLigence to detect cytotoxicity effect of Epstein-Barr virus latent membrane protein 2 (EBV LMP2)-activated $CD8^+$ T cells against LMP2-expressing target cells [38]. Similar to what we observed in NK cells, T:E ratio was a crucial determinant for the protective effect of these cytotoxic lymphocytes, with target cells unaffected at low doses of activated $CD8^+$ T cells.

NK cells were first transfused into acute myeloid leukaemia patients to exert graft-versus-leukaemia reactions [39]. The success of NK cell treatment in haematological cancers at clinical settings encouraged its use against solid cancers in preclinical studies involving ovarian cancer, glioblastoma and colorectal cancer PDXs, and in clinical trials for melanoma, head and neck squamous cell carcinoma and gastrointestinal cancer [40–43]. Tumour cells often have deregulated major histocompatibility (MHC) class I expression leading to immune surveillance escape by $CD8^+$ T cells. As MHC class I molecules are ligands for NK cell inhibitory receptors, its absence in tumour cells presents a "kill me" signal to NK cells. Besides cytotoxicity, NK cells are involved in tumour inflammation by producing various chemokines and cytokines [43,44].

NK-92 (CRL-2407) is an immortal NK cell line derived from the PBMCs of a non-Hodgkins lymphoma patient. Its high cytotoxic potential against tumour cell lines (solid and liquid tumours) and non-tumour cells makes it a good source of immune effector cells that can be cultured and expanded [21,22,45]. Maki et al. and Klingemann et al. had written extensively on its immunophenotype characterisations, cytotoxicity functional properties, and usage in preclinical studies as well as in clinical trials [13,46,47]. ATCC, the source of our NK-92, had also immunophenotyped the cells (https://www.atcc.org/products/crl-2407). The absence of CD16 expression in NK-92 cells makes them attractive as a study model to look at direct cell-mediated cytotoxicity without any participation of ADCC. NK-92's high cytolytic ability has been partially related to its high expression of varied activating receptors such as NKp30, NKp46 and NKG2D, while only retaining a low level of inhibitory receptors for eg. KIR2DL4 and NKG2A/B [46].

Despite the immortality, NK-92 requires fastidious care and maintenance to preserve its viability and cell-killing effect. Firstly, its cryopreservation is best in the vapour phase of liquid nitrogen, as recommended by ATCC. Thawed NK-92 cells from the liquid phase of liquid nitrogen did not grow and aggregate after a few passages *in vitro* (data not shown). Secondly, these cells should be maintained and passaged at the suggested concentration and interval in order to maintain their growth in aggregate form. Overgrowth of NK-92 leads to dispersal problem during subculture and less accurate cell counts. Passaging of undergrowing cells causes poor viability and cell aggregation in subsequent generations of NK-92. Also, the addition of cytokine IL-2 in its media is of utmost importance for the aggregate formation and their overall growth. NK-92 cells that do not form aggregates within a day or two after passaging, have poor viability *in vitro*, and ultimately, lose their cytotoxic ability.

Most NPC biological-based research has either utilised cell lines or PDXs established from fresh patient biopsies. This is mainly due to the facts that the malignancy is highly treatable with radio-chemotherapy and the nasopharynx is a difficult site to be operated on. Unfortunately, most oft-used NPC cell lines are reportedly somatic cell hybrids of HeLa (a cervical cancer cell line), containing human papilloma virus instead of Epstein-Barr virus, or are highly similar to each other [30,48]. PDXs, on the other hand, contain NPC cells that are more recapitulative to actual tumour cells albeit with an absence of human immune cells, and have been increasingly used to personalise cancer therapeutics, in preclinical drug development, and to study basic cancer biology and immunotherapy [49–51]. Thus, it is not surprising to find that the NPC PDX cells in our study were more sensitive to NK-92 cytotoxicity than HK1 cell line which was established in 1980 and is one of the most cultured NPC cells [24]. Despite their more sensitive nature, NPC PDX cells were found to be fairly robust and were able to proliferate just as well in co-culture media as in their individual medium. Furthermore, these cells were easily transducible via lentivirus to incorporate GFP for therapeutic and cancer cell modelling studies as shown here, and elsewhere [28].

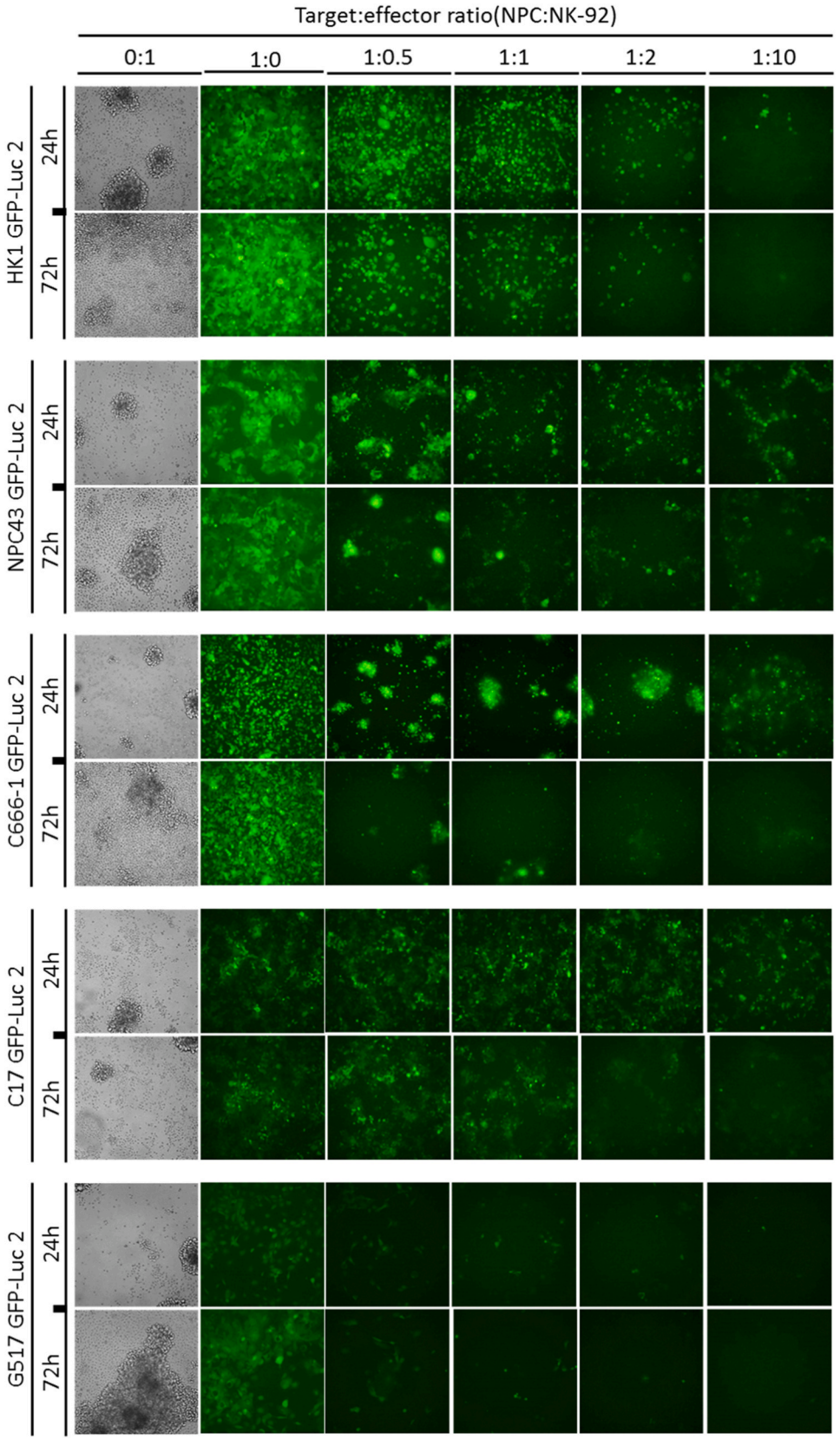

(caption on next page)

Fig. 9. GFP-based microscopy. The GFP-transduced target cells (A) HK1, NPC43, (B) C666–1 and C17 were co-cultured with effector NK-92 cells. Images were acquired after 24 and 72 h of co-culture. 10× objective.

Tumour-infiltrating lymphocytes (TILs) are predominantly located within the tumour cell nests and in the stroma of NPC [52,53]. Amongst which, increased levels of NK cells were reportedly found in advanced stages and their densities also significantly correlated with improved overall survival and progression-free survival in NPC patients [2]. Combined presence of NK and mast cells was also a predictor of NPC recurrence or metastasis. Together, these findings and NK cells' innate ability to eliminate tumour cells without prior sensitization provide a strong basis for exploring the biological use of NK cells in NPC immunotherapy. At least two groups had performed in-depth experiments to define possible mechanisms involved in the cytokilling process of NK cells in NPC cell lines and PDXs in recent years [8,9,54]. They measured cellular cytotoxicity via an endpoint assay to detect the release of either a cytosolic enzyme, lactate dehydrogenase, or a fluorescent compound, calcein, upon damage of the plasma membrane. While both assays were relatively cheaper to use in comparison to xCELLigence platform, their main drawback is total laboratory hands-on time and experience required for their protocols. We find that the label-free detection, minimal handling and hands-on time spent to run above NK-92 cytotoxicity experiments are very advantageous to minimise physiological and run-to-run variabilities. The limitations of our study include no HLA matching was performed on the NPC cell lines and PDX lines prior to co-culture with NK-92, and NK-92 cells are unsuitable for studies looking into ADCC due to an absence of CD16 expression.

5. Conclusion

We have shown that NPC cell lines and PDX lines responded differently to NK-92 cells via xCELLigence RTCA platform, whereby cell lines were less sensitive to the presence of NK-92 and recorded higher KT50 values than PDX lines, especially seen in the lower T:E ratios. Reduced impedance, equivalent to poorer cell viability, of target NPC cells in co-culture experiments was not due to the co-culture media used. Similar patterns of cell viability as a result of cytotoxicity were reproduced in fluorescence microscopy using GFP-transduced NPC cells.

Author contribution statement

Marini Marzuki: Conceived and designed the experiments; Performed the experiments; Analyzed and interpreted the data; Contributed reagents, materials, analysis tools or data; Wrote the paper.

Susan Ling Hoe: Conceived and designed the experiments; Analyzed and interpreted the data; Wrote the paper.

Fatin Nur Asyiqin Abd Talib: Performed the experiments; Analyzed and interpreted the data; Wrote the paper.

Data availability statement

Data included in article/supp. material/referenced in article.

Declaration of competing interest

The authors declare that they have no known competing financial interests or personal relationships that could have appeared to influence the work reported in this paper.

Acknowledgements

We would like to thank the Director General of Health Malaysia for his permission to publish this article. This study was supported by a research grant from the Ministry of Health Malaysia (NMRR-18-596-41153). We are grateful to the former leadership of Alan Soo-Beng Khoo. We also thank Tan Lu Ping and Munirah Ahmad for their critical reviews, and past and present members of Molecular Pathology Unit, Cancer Research Centre, IMR for their technical and scientific support/discussion.

Appendix A. Supplementary data

Supplementary data to this article can be found online at https://doi.org/10.1016/j.heliyon.2023.e17480.

References

[1] H. Sung, J. Ferlay, R.L. Siegel, M. Laversanne, I. Soerjomataram, A. Jemal, et al., Global cancer statistics 2020: GLOBOCAN estimates of incidence and mortality worldwide for 36 cancers in 185 countries, CA Cancer J. Clin. 71 (2021) 209–249. https://onlinelibrary.wiley.com/doi/10.3322/caac.21660.

[2] J. Lu, X.-M. Chen, H.-R. Huang, F.-P. Zhao, F. Wang, X. Liu, et al., Detailed analysis of inflammatory cell infiltration and the prognostic impact on nasopharyngeal carcinoma, Head Neck 40 (6) (2018) 1245–1253. https://onlinelibrary.wiley.com/doi/10.1002/hed.25104.

[3] J.K. Chan, P. Slootweg, Tumours of the nasopharynx, in: A.K. El-Naggar, J.K.C. Chan, J.R. Grandis, T. Takata, P.J. Slootweg (Eds.), WHO Classification of Head and Neck Tumours: WHO Classification of Tumours, fourth ed., IARC Press, 2017, pp. 63–76.

[4] Y. Shen, S. Zhang, R. Sun, T. Wu, J. Qian, Understanding the interplay between host immunity and Epstein-Barr virus in NPC patients, Emerg. Microbes Infect. 4 (1) (2015) 1–9, https://doi.org/10.1038/emi.2015.20.

[5] A.Z.E. Lee, L.S.Y. Tan, C.M. Lim, Cellular-based immunotherapy in Epstein-Barr virus induced nasopharyngeal cancer, Oral Oncol 84 (2018) 61–70, https://doi.org/10.1016/j.oraloncology.2018.07.011.

[6] H. Dianat-Moghadam, M. Rokni, F. Marofi, Y. Panahi, M. Yousefi, Natural killer cell–based immunotherapy: from transplantation toward targeting cancer stem cells, J. Cell Physiol 234 (1) (2019) 259–273. https://onlinelibrary.wiley.com/doi/10.1002/jcp.26878.

[7] S.K. Grossenbacher, E.G. Aguilar, W.J. Murphy, Leveraging natural killer cells for cancer immunotherapy, Immunotherapy 9 (6) (2017) 487–497. https://www.futuremedicine.com/doi/10.2217/imt-2017-0013.

[8] A. Makowska, T. Braunschweig, B. Denecke, L. Shen, V. Baloche, P. Busson, et al., Interferon β and anti-PD-1/PD-L1 checkpoint blockade cooperate in NK cell-mediated killing of nasopharyngeal carcinoma cells, Transl. Oncol. 12 (9) (2019) 1237–1256, https://doi.org/10.1016/j.tranon.2019.04.017.

[9] A. Makowska, S. Meier, L. Shen, P. Busson, V. Baloche, U. Kontny, Anti-PD-1 antibody increases NK cell cytotoxicity towards nasopharyngeal carcinoma cells in the context of chemotherapy-induced upregulation of PD-1 and PD-L1, Cancer Immunol. Immunother. 70 (2) (2021) 323–336, https://doi.org/10.1007/s00262-020-02681-x.

[10] N. Shimasaki, A. Jain, D. Campana, NK cells for cancer immunotherapy, Nat. Rev. Drug. Discov. 19 (3) (2020), https://doi.org/10.1038/s41573-019-0052-1, 200–18.

[11] Y.T. Png, A.Z.Y. Yang, M.Y. Lee, M.J.M. Chua, C.M. Lim, The role of NK cells in EBV infection and EBV-associated NPC, Viruses 13 (2) (2021) 1–22.

[12] T. Tonn, S. Becker, R. Esser, D. Schwabe, E. Seifried, Cellular immunotherapy of malignancies using the clonal natural killer cell line NK-92, J. Hematother. Stem Cell Res. 10 (4) (2001) 535–544. https://www.liebertpub.com/doi/10.1089/15258160152509145.

[13] H.-G. Klingemann, J. Martinson, Ex vivo expansion of natural killer cells for clinical applications, Cytotherapy 6 (1) (2004) 15–22, https://doi.org/10.1080/14653240310004548.

[14] L. Navarrete-Galvan, M. Guglielmo, J. Cruz Amaya, J. Smith-Gagen, V.C. Lombardi, R. Merica, et al., Optimizing NK-92 serial killers: gamma irradiation, CD95/Fas-ligation, and NK or LAK attack limit cytotoxic efficacy, J. Transl. Med. 20 (1) (2022) 151, https://doi.org/10.1186/s12967-022-03350-6.

[15] J. Chu, F. Gao, M. Yan, S. Zhao, Z. Yan, B. Shi, et al., Natural killer cells: a promising immunotherapy for cancer, J. Transl. Med. 20 (1) (2022) 240, https://doi.org/10.1186/s12967-022-03437-0.

[16] T.J. Laskowski, A. Biederstädt, K. Rezvani, Natural killer cells in antitumour adoptive cell immunotherapy, Nat. Rev. Cancer 22 (10) (2022) 557, 75, https://www.nature.com/articles/s41568-022-00491-0.

[17] F. Rossi, N. Fredericks, A. Snowden, M.J. Allegrezza, U.Y. Moreno-Nieves, Next generation natural killer cells for cancer immunotherapy, Front. Immunol. 13 (2022) 1–19. https://www.frontiersin.org/articles/10.3389/fimmu.2022.886429/full.

[18] M. Felices, T.R. Lenvik, Z.B. Davis, J.S. Miller, D.A. Vallera, Generation of BiKEs and TriKEs to improve NK cell-mediated targeting of tumor cells, in: Methods in Molecular Biology, 2016, pp. 333–346. http://link.springer.com/10.1007/978-1-4939-3684-7_28.

[19] S.S. Tay, H. Carol, M. Biro, TriKEs and BiKEs join CARs on the cancer immunotherapy highway, Hum. Vaccin. Immunother 12 (11) (2016) 2790–2796, https://doi.org/10.1080/21645515.2016.1198455.

[20] O. Demaria, L. Gauthier, G. Debroas, E. Vivier, Natural killer cell engagers in cancer immunotherapy: next generation of immuno-oncology treatments, Eur. J. Immunol. 51 (8) (2021), 1934–42. Available from: https://onlinelibrary.wiley.com/doi/10.1002/eji.202048953.

[21] S. Grote, K.C. Chan, C. Baden, H. Bösmüller, M. Sulyok, L. Frauenfeld, et al., CD276 as a novel CAR NK-92 therapeutic target for neuroblastoma, Adv. CELL GENE Ther. 4 (1) (2021) 1–15. https://onlinelibrary.wiley.com/doi/10.1002/acg2.105.

[22] M.H. Abumaree, N.A. Alshehri, A. Almotery, A.M. Al Subayyil, E. Bahattab, F.M. Abomaray, et al., Preconditioning human natural killer cells with chorionic villous mesenchymal stem cells stimulates their expression of inflammatory and anti-tumor molecules, Stem Cell Res. Ther. 10 (1) (2019) 50. https://stemcellres.biomedcentral.com/articles/10.1186/s13287-019-1153-9.

[23] F. Fasbender, C. Watzl, Impedance-based analysis of Natural Killer cell stimulation, Sci. Rep. 8 (1) (2018) 4938, https://doi.org/10.1038/s41598-018-23368-5.

[24] D.P. Huang, J.H. Ho, Y.F. Poon, E.C. Chew, D. Saw, M. Lui, et al., Establishment of a cell line (NPC/HK1) from a differentiated squamous carcinoma of the nasopharynx, Int. J. Cancer 26 (2) (1980) 127–132. http://www.ncbi.nlm.nih.gov/entrez/query.fcgi?cmd=Retrieve&db=PubMed&dopt=Citation&list_uids=6259064.

[25] W. Lin, Y.L. Yip, L. Jia, W. Deng, H. Zheng, W. Dai, et al., Establishment and characterization of new tumor xenografts and cancer cell lines from EBV-positive nasopharyngeal carcinoma, Nat. Commun. 9 (1) (2018).

[26] Y.L. Yip, W. Lin, W. Deng, L. Jia, K.W. Lo, P. Busson, et al., Establishment of a nasopharyngeal carcinoma cell line capable of undergoing lytic Epstein–Barr virus reactivation, Lab Investig. 98 (8) (2018) 1093–1104, https://doi.org/10.1038/s41374-018-0034-7.

[27] A.B. Hui, S.T. Cheung, Y. Fong, K.W. Lo, D.P. Huang, Characterization of a new EBV-associated nasopharyngeal carcinoma cell line, Cancer Genet. Cytogenet. 101 (2) (1998) 83–88. http://www.ncbi.nlm.nih.gov/pubmed/9494607.

[28] S.-Y. Teow, K. Liew, M.F. Che Mat, M. Marzuki, N. Abdul Aziz, T.-L. Chu, et al., Development of a luciferase/luciferin cell proliferation (XenoLuc) assay for real-time measurements of Gfp-Luc2-modified cells in a co-culture system, BMC Biotechnol. 19 (1) (2019) 34. https://bmcbiotechnol.biomedcentral.com/articles/10.1186/s12896-019-0528-4.

[29] RTCA Software Pro Software Manual. version 1, Agilent Technologies (ACEA Biosciences, Inc.), 2019, p. 142.

[30] S.Y.Y. Chan, K.W. Choy, S.W. Tsao, Q. Tao, T. Tang, G.T.Y. Chung, et al., Authentication of nasopharyngeal carcinoma tumor lines, Int. J. Cancer 122 (9) (2008) 2169–2171.

[31] C.-H. Chiu, K.F. Lei, W.-L. Yeh, P. Chen, Y.-S. Chan, K.-Y. Hsu, et al., Comparison between xCELLigence biosensor technology and conventional cell culture system for real-time monitoring human tenocytes proliferation and drugs cytotoxicity screening, J. Orthop. Surg. Res. 12 (1) (2017) 149. http://josr-online.biomedcentral.com/articles/10.1186/s13018-017-0652-6.

[32] X. Wang, X. Yang, C. Zhang, Y. Wang, T. Cheng, L. Duan, et al., Tumor cell-intrinsic PD-1 receptor is a tumor suppressor and mediates resistance to PD-1 blockade therapy, Proc. Natl. Acad. Sci. India 117 (12) (2020), 6640–50, https://pnas.org/doi/full/10.1073/pnas.1921445117.

[33] J. Stefanowicz-Hajduk, J.R. Ochocka, Real-time cell analysis system in cytotoxicity applications: usefulness and comparison with tetrazolium salt assays, Toxicol. Reports (2020) 335–344, https://doi.org/10.1016/j.toxrep.2020.02.002.

[34] J. Martinez-Serra, A. Gutierrez, M. Navarro-Palou, T. Ros, J.C. Amat, T.F. Marcus, et al., xCELLigence system for real-time label-free monitoring of growth and viability of cell lines from hematological malignancies, Onco. Targets Ther. 7 (2014) 985. http://www.dovepress.com/xcelligence-system-for-real-time-label-free-monitoring-of-growth-and-v-peer-reviewed-article-OTT.

[35] M. Daker, J. Yeo, N. Bakar, A.S.A. Abdul Rahman, M. Ahmad, T.C. Yeo, et al., Inhibition of nasopharyngeal carcinoma cell proliferation and synergism of cisplatin with silvestrol and episilvestrol isolated from Aglaia stellatopilosa, Exp. Ther. Med. 11 (6) (2016) 2117–2126.

[36] R. Kan, W.H. Shuen, H.L. Lung, A.K.L. Cheung, W. Dai, D.L.W. Kwong, et al., NF-κB p65 subunit is modulated by latent transforming growth factor-β binding protein 2 (LTBP2) in nasopharyngeal carcinoma HONE1 and HK1 cells, PLoS One 10 (5) (2015) 1–21.

[37] A. Wu, L. Zhang, N. Luo, L. Zhang, L. Li, Q. Liu, Limb-bud and heart (LBH) inhibits cellular migration, invasion and epithelial-mesenchymal transition in nasopharyngeal carcinoma via downregulating αB-crystallin expression, Cell. Signal. 85 (2021), 110045.

[38] Y. Ge, Z. Zhou, X. Wang, Y. Zhou, W. Liu, Z. Teng, et al., In vitro evaluation of the therapeutic effectiveness of EBV-LMP2 recombinant adenovirus vaccine in nasopharyngeal carcinoma, Biomed. Pharmacother. 121 (2020), 109626, https://doi.org/10.1016/j.biopha.2019.109626.

[39] L. Ruggeri, M. Capanni, M. Casucci, I. Volpi, A. Tosti, K. Perruccio, et al., Role of natural killer cell alloreactivity in HLA-mismatched hematopoietic stem cell transplantation, Blood 94 (1) (1999) 333–339, https://doi.org/10.1182/blood.V94.1.333.413a31_333_339.

[40] M.A. Geller, D.A. Knorr, D.A. Hermanson, L. Pribyl, L. Bendzick, V. Mccullar, et al., Intraperitoneal delivery of human natural killer cells for treatment of ovarian cancer in a mouse xenograft model, Cytotherapy 15 (10) (2013) 1297–1306. https://www.sciencedirect.com/science/article/pii/S1465324913005598.

[41] A. Gras Navarro, J. Kmiecik, L. Leiss, M. Zelkowski, A. Engelsen, Bruserud Ø, et al., NK cells with KIR2DS2 immunogenotype have a functional activation advantage to efficiently kill glioblastoma and prolong animal survival, J Immunol. 193 (12) (2014) 6192–6206, https://doi.org/10.4049/jimmunol.1400859.
[42] J.P. Veluchamy, S. Lopez-Lastra, J. Spanholtz, F. Bohme, N. Kok, D.A.M. Heideman, et al., Vivo efficacy of umbilical cord blood stem cell-derived NK cells in the treatment of metastatic colorectal cancer, Front Immunol. 8 (2017) 87. http://journal.frontiersin.org/article/10.3389/fimmu.2017.00087/full.
[43] S. Maddineni, J.L. Silberstein, J.B. Sunwoo, Emerging NK cell therapies for cancer and the promise of next generation engineering of iPSC-derived NK cells, J. Immunother. Cancer 10 (5) (2022), e004693. http://jitc.bmj.com/content/10/5/e004693.abstract.
[44] N. Du, F. Guo, Y. Wang, J. Cui, NK cell therapy: a rising star in cancer treatment, Cancers (Basel) 13 (16) (2021) 4129. https://www.mdpi.com/2072-6694/13/16/4129.
[45] F. Cerignoli, Y.A. Abassi, B.J. Lamarche, G. Guenther, D. Santa Ana, D. Guimet, et al., In vitro immunotherapy potency assays using real-time cell analysis, PLoS One 13 (3) (2018), e0193498. Kanellopoulos J, https://dx.plos.org/10.1371/journal.pone.0193498.
[46] G. Maki, H.-G. Klingemann, J.A. Martinson, Y.K. Tam, Factors regulating the cytotoxic activity of the human natural killer cell line, NK-92, J. Hematother. Stem Cell Res. 10 (3) (2001) 369–383. https://linkinghub.elsevier.com/retrieve/pii/0308595377901209.
[47] H. Klingemann, L. Boissel, F. Toneguzzo, Natural killer cells for immunotherapy - advantages of the NK-92 cell line over blood NK cells, Front. Immunol. 7 (2016) 1–7.
[48] M.J. Strong, M. Baddoo, A. Nanbo, M. Xu, A. Puetter, Z. Lin, Comprehensive high-throughput RNA sequencing analysis reveals contamination of multiple nasopharyngeal carcinoma cell lines with HeLa cell genomes, J. Virol. 88 (18) (2014) 10696–10704. http://www.ncbi.nlm.nih.gov/pubmed/24991015.
[49] J. Lang, N. Weiss, B.M. Freed, R.M. Torres, R. Pelanda, Generation of hematopoietic humanized mice in the newborn BALB/c-Rag2null Il2rγnull mouse model: a multivariable optimization approach, Clin. Immunol. 140 (1) (2011) 102–116.
[50] J. Lang, B. Zhang, M. Kelly, J.N. Peterson, J. Barbee, B.M. Freed, et al., Replacing mouse BAFF with human BAFF does not improve B-cell maturation in hematopoietic humanized mice, Blood Adv. 1 (27) (2017) 2729–2741. https://ashpublications.org/bloodadvances/article/1/27/2729/15837/Replacing-mouse-BAFF-with-human-BAFF-does-not.
[51] J. Bhimani, K. Ball, J. Stebbing, Patient-derived xenograft models—the future of personalised cancer treatment, Br. J. Cancer 122 (5) (2020), 601–2, https://www.nature.com/articles/s41416-019-0678-0.
[52] Y. Zong, C. Zhang, F. Zhang, J. Kuan, M. Chen, K. Feng, et al., Infiltrating lymphocytes and accessory cells in nasopharyngeal carcinoma, Japanese J. Cancer Res. 84 (8) (1993) 900. –5, http://www.ncbi.nlm.nih.gov/pubmed/8407554.
[53] B.A. Berele, Y. Cai, G. Yang, Prognostic value of tumor infiltrating lymphocytes in nasopharyngeal carcinoma patients: meta-analysis, Technol Cancer Res Treat 20 (2021), 153303382110342. http://journals.sagepub.com/doi/10.1177/15330338211034265.
[54] C. Zhao, Y. Liu, Z. Liang, H. Feng, S. Xu, MACC1 facilitates the escape of nasopharyngeal carcinoma cells from killing by natural killer cells, Biotechnol. Biotechnol. Equip 33 (1) (2019) 579–588, https://doi.org/10.1080/13102818.2019.1596041.